

Article

# First Report of the Marine Benthic Dinoflagellate *Bysmatrum subsalsum* from Korean Tidal Pools

Joon Sang Park <sup>1,†</sup>, Zhun Li <sup>2,†</sup> , Hyun Jung Kim <sup>1,3</sup>, Ki Hyun Kim <sup>2</sup>, Kyun Woo Lee <sup>4,\*</sup> , Joo Yeon Youn <sup>1</sup>,  
Kyeong Yoon Kwak <sup>1</sup> and Hyeon Ho Shin <sup>1,\*</sup>

<sup>1</sup> Library of Marine Samples, Korea Institute of Ocean Science & Technology, Geoje 53201, Korea; jspark1101@kiost.ac.kr (J.S.P.); guswjd9160@kiost.ac.kr (H.J.K.); yjy5225@kiost.ac.kr (J.Y.Y.); kky3827@kiost.ac.kr (K.Y.K.)

<sup>2</sup> Biological Resource Center/Korean Collection for Type Cultures (KCTC), Korea Research Institute of Bioscience and Biotechnology, Jeongeup 56212, Korea; lizhun@kribb.re.kr (Z.L.); kimkh@kribb.re.kr (K.H.K.)

<sup>3</sup> Department of Oceanography, Pukyong National University, Yongso-ro, Busan 48513, Korea

<sup>4</sup> Marine Biotechnology Research Center, Korea Institute of Ocean Science & Technology, Busan 49111, Korea

\* Correspondence: kyunu@kiost.ac.kr (K.W.L.); shh961121@kiost.ac.kr (H.H.S.); Tel.: +82-51-664-3318 (K.W.L.); +82-55-639-8440 (H.H.S.); Fax: +82-55-639-8429 (H.H.S.)

† Joon-Sang Park and Zhun Li contributed equally as co-first authors.

**Abstract:** Dense patches were observed in the tidal pools of the southern area of Korea. To clarify the causative organisms, the cells were collected and their morphological features were examined using light and scanning electron microscopy (SEM). In addition, after establishing strains for the cells the molecular phylogeny was inferred with concatenated small subunit (SSU) and large subunit (LSU) rRNA sequences. The cells were characterized by a nucleus in the hypotheca, strong reticulations in thecal plates, the separation of plates 2a and 3a, the tear-shaped apical pore complex, an elongated rectangular 1a plate and the absence of the right sulcal list. The thecal plate formula was  $Po, X, 4', 3a, 7'', 6c, 4S, 5''', 2''''$ . Based on these morphological features, the cells were identified as *Bysmatrum subsalsum*. In the culture, the spherical cysts of *B. subsalsum* without thecal plates were observed. Molecular phylogeny revealed two ribotypes of *B. subsalsum* are identified; The Korean isolates were nested within the ribotype B consisting of the isolates from China, Malaysia and the French Atlantic, whereas the ribotype A includes only the isolates from the Mediterranean Sea. In the phylogeny, *B. subsalsum* and *B. austrafurum* were grouped. This can be supported by the morphological similarity between the two species, indicating that the two species may be conspecific, however *B. subsalsum* may distinguish from *B. austrafurum*, because of differences in the types of eyespots reported in previous studies. These findings support the idea that there is cryptic diversity within *B. subsalsum*.

**Keywords:** *Bysmatrum*; cyst; eyespot; morphology; ribotype



**Citation:** Park, J.S.; Li, Z.; Kim, H.J.; Kim, K.H.; Lee, K.W.; Youn, J.Y.; Kwak, K.Y.; Shin, H.H. First Report of the Marine Benthic Dinoflagellate *Bysmatrum subsalsum* from Korean Tidal Pools. *J. Mar. Sci. Eng.* **2021**, *9*, 649. <https://doi.org/10.3390/jmse9060649>

Academic Editor: Carmela Caroppo

Received: 17 May 2021

Accepted: 8 June 2021

Published: 12 June 2021

**Publisher's Note:** MDPI stays neutral with regard to jurisdictional claims in published maps and institutional affiliations.



**Copyright:** © 2021 by the authors. Licensee MDPI, Basel, Switzerland. This article is an open access article distributed under the terms and conditions of the Creative Commons Attribution (CC BY) license (<https://creativecommons.org/licenses/by/4.0/>).

## 1. Introduction

The genus *Bysmatrum* M.A. Faust and K.A. Steidinger was erected to separate three benthic *Scrippsiella* species, *Scrippsiella arenicola* T. Horiguchi and R.N. Pienaar, *S. subsalsa* (Ostenfeld) K.A. Steidinger and Balech and *S. caponii* T. Horiguchi and R.N. Pienaar [1]. These species share a number of morphological characterizations of thecal plates: a lack of contact between 2a and 3a, the presence of six cingular plates, and the posterior sulcal plate that does not touch the cingulum [1]. Based on such morphological characteristics, six *Bysmatrum* species (including *Bysmatrum subsalsum* (Ostenfeld) M.A. Faust and K.A. Steidinger as the type species have been reported so far [1–6] and, within the genus, the *Bysmatrum* species) can be distinguished from each other by the differences in cell size and shape, plate ornamentation, cingulum displacement, the morphology of the apical pore complex (APC), nucleus position, habitat and habitus [1,4,5,7,8]. However, molecular data for *Bysmatrum* species are as yet available for only five species; *B. arenicola* T. Horiguchi and R. N. Pienaar, *B. austrafurum* Dawut, Sym, Suda and Horiguchi, *B. granulorum* L. Ten-Hage,

J.P. Quod, J. Turquet and Couté, *B. gregarium* (E. H. Lombard and B. Capon) T. Horiguchi and Hoppenrath and *B. subsalsum* [6–9].

Since the morphological descriptions of *Bysmatrum* species by Faust and Steidinger [1], Anglès et al. [7] documented the morphological details and molecular phylogeny of *B. subsalsum* collected from different locations of the Mediterranean Basin, and concluded that the strains of *B. subsalsum* are morphologically indistinguishable but genetically distinct, probably due to the differences in habitat, physiology or life-history traits. Since then, Luo et al. [8] documented that *B. subsalsum* strains from Malaysia and the French Atlantic formed a subclade (ribotype B) that can be distinguished from a clade (ribotype A) consisting of strains from the Mediterranean Sea and that there is cryptic diversity within *B. subsalsum*, based on the genetic distance shown in ITS sequences among *Bysmatrum* species [7]. This indicates that additional molecular data (including morphological descriptions) are needed to clarify the cryptic diversity of *B. subsalsum*, with strains established from water bodies of various geographical regions.

*Bysmatrum subsalsum* is a cosmopolitan species [10], and its occurrences have been recorded in the Aral Sea, the Mediterranean Sea, the Caribbean Sea, the Gulf of Mexico, the French and Portuguese Atlantic coast and the East and South China Sea [7,8]. However, in the Korean coastal area, this species has not been found, and only *B. gregarium* (as *B. caponii*) isolated from plankton samples has been recorded, with its morphology and molecular information [9]. In the tidal pools of the southern area of Korea, we observed dense patches caused by unidentified organisms. These were isolated, and strains were established and the morphological features were examined using light and scanning electron microscopy (SEM). The observations revealed that the species was identical to *B. subsalsum*. In this study, we describe the morphological details of Korean strains of *B. subsalsum* and report on their molecular characterization, based on concatenated small subunit (SSU) and large subunit (LSU) rRNA gene sequences.

## 2. Materials and Methods

### 2.1. Sampling and Culture

In June 2017, dense patches of phytoplankton were observed in the tidal pools of Geoje Island (34°59'34.3" N, 128°41'44.1" E) and Jeju Island (33°29'26.5" N, 126°25'12.8" E), Korea. Water temperature and salinity were 23.0 °C and 34 psu in the tidal pool of Geoje Island, and 10.5 °C and 24.5 psu in the tidal pool of Jeju Island, respectively. The water samples from the pools were collected using the 50 mL conical tubes and were then transported to the laboratory for observation of the causative organism. In the laboratory, the single mass colonies from the samples were isolated using a glass micropipette on an inverted microscope (Eclipse Ts2R, Nikon, Tokyo, Japan), and transferred into a 24-well tissue plate containing f/2 medium adjusted to a salinity of 32. The isolated colonies were maintained at 24 °C in a 12:12 LD cycle under a photon irradiance of 100  $\mu\text{mol photons}\cdot\text{m}^{-2}\cdot\text{s}^{-1}$ . After sufficient growth, the cells were transferred to a culture flask. A monoclonal culture was successfully established from the cells collected in the tidal pool of Geoje Island and deposited in the Library of Marine Samples, Korea Institute of Ocean Science and Technology, as strain number LIMS-PS-2685 (=MABIK PD00002006). The isolate from the tidal pool of Jeju Island was also established as a strain; however, it is currently unavailable because of unexpected cell death.

### 2.2. Morphological Observation

Live cells were isolated and photographed at 1000X magnification using an AxioCam 512c digital camera (Carl Zeiss, Göttingen, Germany) on an upright microscope (Zeiss Axio Imager2, Carl Zeiss, Göttingen, Germany). For fluorescence microscopy, approximately 1 mL of cell culture was transferred to a 1.5-mL microcentrifuge tube, and 4',6-diamidino-2-phenylindole (DAPI) stain (Sigma-Aldrich, St. Louis, MO, USA) was added at a final concentration of 10  $\mu\text{g mL}^{-1}$ . Cells were then incubated in the dark at room temperature

for 1 h, and viewed and photographed through a Zeiss Filterset 49 (emission: BP 365–445; beamsplitter: FT 395).

For scanning electron microscopy, a 20 mL aliquot of a dense culture was fixed in glutaraldehyde and paraformaldehyde with a final concentration of 2% (*w/v*). The aliquot containing fixed cells was filtered through a polycarbonate membrane filter (5 µm pore size), without applying additional pressure and rinsed three times with distilled water to remove the salt. After rinsing, the sample was dehydrated in an ethanol series (10, 30, 50, 70, 90 and 100% ethanol, followed by two 100% ethanol steps) and dried using a critical point dryer (BAL-TEC, CPD 300, Balzers, Germany). Finally, the sample was coated with gold-palladium and examined using a field emission-scanning electron microscope (JSM-7610F, Jeol, Japan).

### 2.3. DNA Extraction and Sequencing

The mass colonies were harvested via centrifugation for 10 min at room temperature, and the supernatant was discarded. Genomic DNA was extracted from cell pellets using a DNeasy Plant Mini Kit (Qiagen, Hilden, Germany), according to the manufacturer's protocol. The SSU rRNA gene was amplified using primers (ATF01: 5'-YAC CTG GTT GAT CCT GCC AGT AG-3' and ATR01: 5'-RMW TGA TCC TTC YGC AGG TTC ACC-3') [11], and the D1–D3 regions of the LSU rRNA gene were amplified using previously described primers (D1R: 5'-ACC CGC TGA ATT TAA GCA TA-3' [12] and 28r691: 5'-CTT GGT CCG TGT TTC AAG AC-3') [11]. PCR reactions were conducted in a volume of 50 µL; 2.0 µL gDNA; 5 µL 10x buffer; 0.2 mM dNTP; 0.1 µM each primer; 0.25 U Taq polymerase (Takara Ex Taq, Takara, Seoul, Korea); and ddH<sub>2</sub>O to a final volume of 50 µL. The PCR condition was as follows: 94 °C for 4 min, 30 cycles of 94 °C for 1 min, 54 °C for 1 min, and 72 °C for 1 min and then 1 extension cycle at 72 °C for 10 min. PCR products were purified with QIAquick PCR purification kit (Qiagen, Hilden, Germany). All rRNA gene sequencing was performed using an ABI PRISM 3700 DNA Analyzer (Applied Biosystems, Foster City, CA, USA). The sequences were trimmed and assembled into contigs using Geneious Prime (<https://www.geneious.com> (accessed on 2 January 2020)).

### 2.4. Phylogenetic Analysis

The sequences were aligned using MAFFT in Geneious plugin with default settings, and some regions manually adjusted using the Geneious Prime. The phylogenetic analysis includes all the published sequences of *Bysmatrum* species. A total of 50 sequences of the order Peridinales were selected, while the family Peridiniaceae and Protoperidiniaceae were used as outgroups. The sequence alignments of SSU and LSU rRNA were concatenated with introduced gaps. The phylogenetic tree for the concatenated sequence alignment was inferred using maximum likelihood (ML) analyses via RAxML version 8 [13], and using Bayesian inference (BI) through MrBayes version 3.2 [14]. The general time reversible (GTR) model with parameters accounting for  $\gamma$ -distributed rate variation across sites (G) was used in all analyses, taking into account 6-class gamma. The GTR+G substitution model was selected using the Akaike information criterion (AIC) as implemented in jModelTest version 2.1.4 [15]. Bootstrap analyses for ML were carried out with 1000 replicates to evaluate statistical reliability. The Markov chain Monte Carlo (MCMC) method for BI was used with four runs for 10 million generations, sampling every 100 generations. The first 10% of trees were deleted as burn-in, and a majority rule consensus tree was constructed to examine the posterior probabilities of each clade. The final trees were visualized with FigTree v1.4.4 (<http://tree.bio.ed.ac.uk/software/figtree/> (accessed on 5 January 2020)).

## 3. Results

### 3.1. Morphology of Vegetative Cell and Resting Cyst of *Bysmatrum subsalsum*

Cells had a conical epitheca and a round hypotheca, were slightly obliquely dorsoventrally flattened and the longitudinal flagella were visible (Figure 1a–f). They were 37–52 µm in length and 31–44 µm in width ( $n = 50$ ). An apical stalk consisting of a transparent gelati-

nous matrix was observed on the apex of the cells (Figure 1b,c). A yellowish eyespot was located on the right side of the sulcus (Figure 1d,e). Rod-shaped chloroplasts were observed in the periphery of the cell (Figure 1g,h). The DAPI-stained nucleus was large, commonly elongated (Figure 1h) and sometimes horseshoe-shaped by the different observation angle (Figure 1i). The position of a nucleus was posteriorly in the hypotheca (Figure 1g–i).

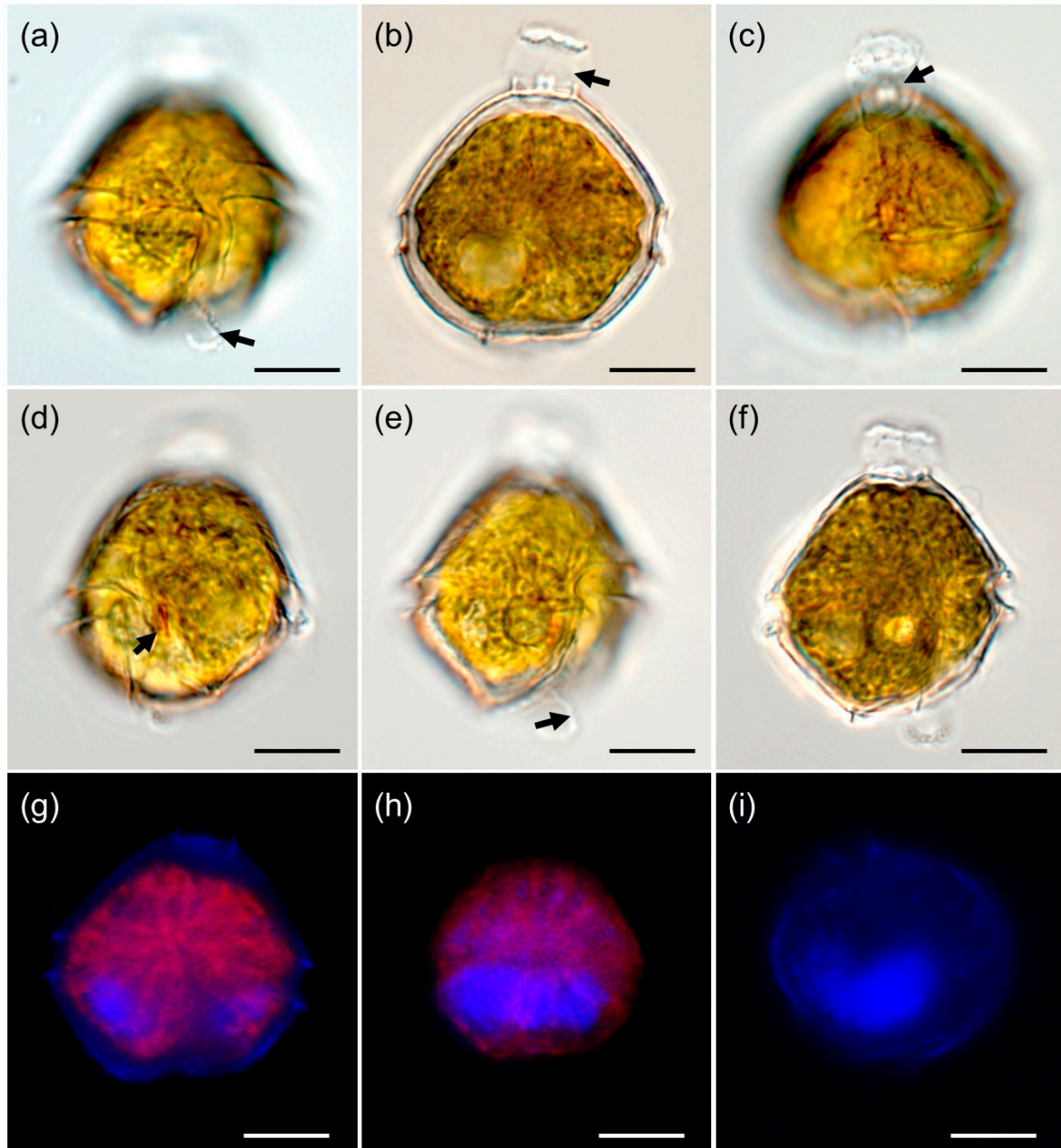


**Figure 1.** Light micrographs of *Bysmatrum subsalsum* (Strain: LIMS-2685). (a) Surface focus of ventral view showing the longitudinal flagella (arrow), sulcus and cingulum. (b) Deeper focus of ventral view showing the outline of the cell and apical stalk (arrow). (c) Surface focus of ventral-apical view showing the apical stalk (arrow). (d) Deeper focus of ventral-lateral view showing a red eyespot (arrow). (e) Surface focus of ventral-right lateral view showing the longitudinal flagella (arrow). (f) Deeper focus of dorsal view. (g) Epifluorescence image of ventral view of DAPI-stained cell showing the position of the nucleus. (h) Epifluorescence image of dorsal view of DAPI-stained cell showing the position of the nucleus. (i) Epifluorescence image of antapical view of DAPI-stained cell showing the shape of the nucleus. Scale bars = 5  $\mu\text{m}$ .

SEM observation revealed that the cells have a plate formula of Po, Cp, X, 4', 3a, 7'', 6C, 4S, 5''', 2'''' (Figure 2). The thecal plates were covered with strong reticulations (Figure 2a–e). Apical pore complex (APC) was tear-shaped and included a Po plate, a round cover plate (Cp) and a canal plate (X) with thick margins formed by the raised borders of the apical plates (Figure 2f). The first apical plate (1') was pentagonal and asymmetrical with shorter anterior sutures than the posterior ones, and surrounded five plates: 2', 4', 1'', 7'' and Sa (Figure 2a,d,e). Three intercalary plates (1a, 2a and 3a) were similar in size, and 1a and 2a contacted each other; however, 3a was separated from 1a and 2a. (Figure 2b,c,e). Plate 1a was elongate and rectangular, whereas plates 2a and 3a were hexagonal and pentagonal, respectively (Figure 2b,c,e). The precingular plates were symmetrically distributed (Figure 2e). The first precingular plate (1'') was pentagonal and smaller than the others (Figure 2a,e). The cingulum was deeply excavated and descended by about one cingulum width (Figure 2a–d). Six cingulum plates were observed; plates C1, C2 and C3 were much smaller than the C4, C5 and C6 plates (Figure 2a–d). In post cingular series, plates 1''', 2''', and 4''' were tetragonal, whereas plates 3''' and 5''' are pentagonal in shape (Figure 2g). The plate 1''' was much smaller than the other plate (Figure 2a–c,g). Two antapical plates (1'''' and 2''') have pentagonal shapes, and plate 2'''' is larger than the 1'''' plate (Figure 2a–c,g). The sulcus was wide and did not contact the antapex (Figure 2a,g), and consisted of four major plates with inconspicuous lists: the anterior sulcal plate (Sa) is narrow and elongated; the left sulcal plate (Sl) in narrow and right sulcal (Sr) plate are triangular (Figure 2a,h); the posterior sulcal plate (Sp) is the largest sulcal plate, wider than long, and does not contact the plate (Figure 2g,h). There were internal sulcal lists (Isl) emerging from left side of the Sr plate (Figure 2h). The left sulcal list (Lsl) that had emerged from the lower side of plate 1''' was visible (Figure 2h).

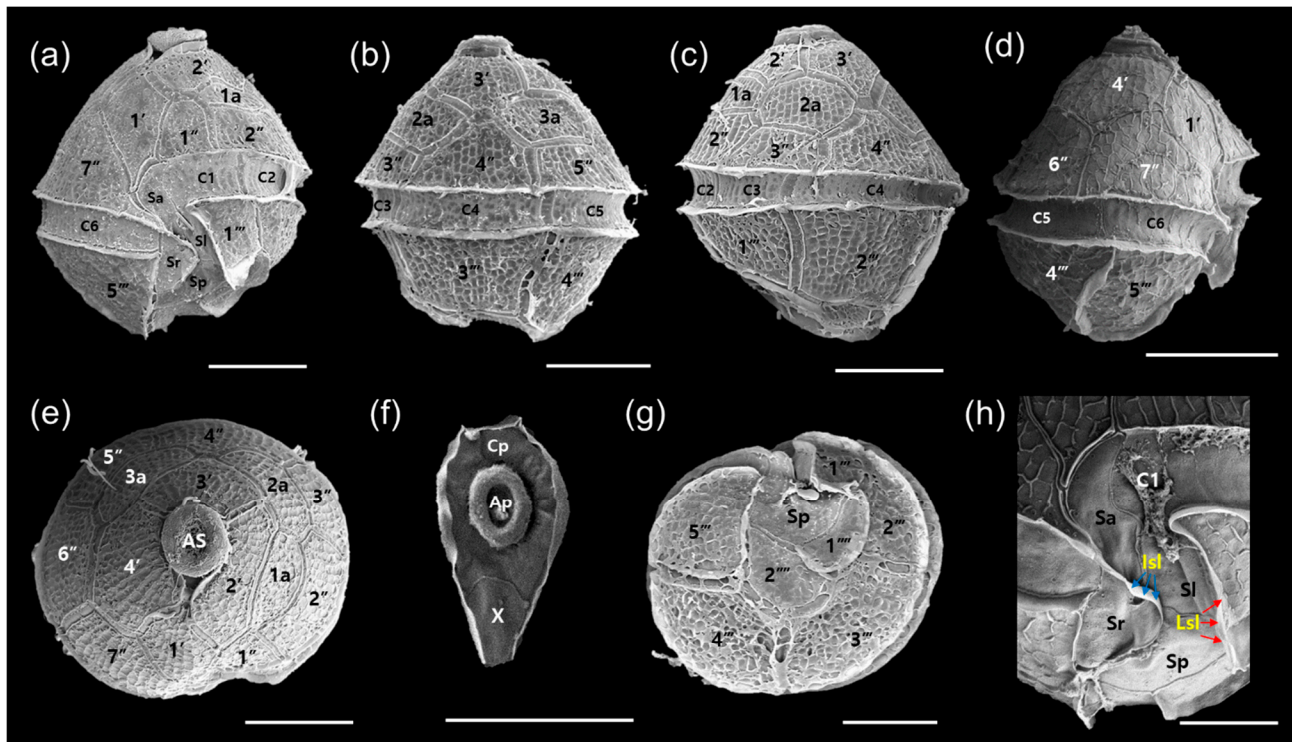


**Figure 2.** Scanning electron micrographs of vegetative cells of *Bysmatrum subsalsum* strain LIMS-2685 from Korea. (a) Ventral view. (b) Dorsal view. (c) Dorsal-left lateral view. (d) Ventral-right lateral view. (e) Apical view, showing a centrally located raised dome (apical stalk: AS) and epithelial plate pattern. (f) Detail of apical pore complex showing the apical pore (AP), cover plate (Cp) and canal plate (X). (g) Antapical view, showing hypothecal plate pattern. (h) Detail of the sulcal plates showing anterior sulcal plate (Sa), right sulcal (Sr) and left sulcal (Sl) plates, posterior sulcal plate (Sp), left (Lsl; red arrows) and internal (Isl; blue arrows) sulcal lists. Scale bars = 10 μm (a–e,g); 5 μm (f,h).

Spherical cysts were observed under culture conditions (Figure 3). The cysts were 29.5–34.6  $\mu\text{m}$  in diameter ( $n = 25$ ). The cyst was grayish in color, and an orange accumulation body was visible (Figure 3a–c). The cyst wall was smooth, without any distinguishing features on the surface (Figure 3d).

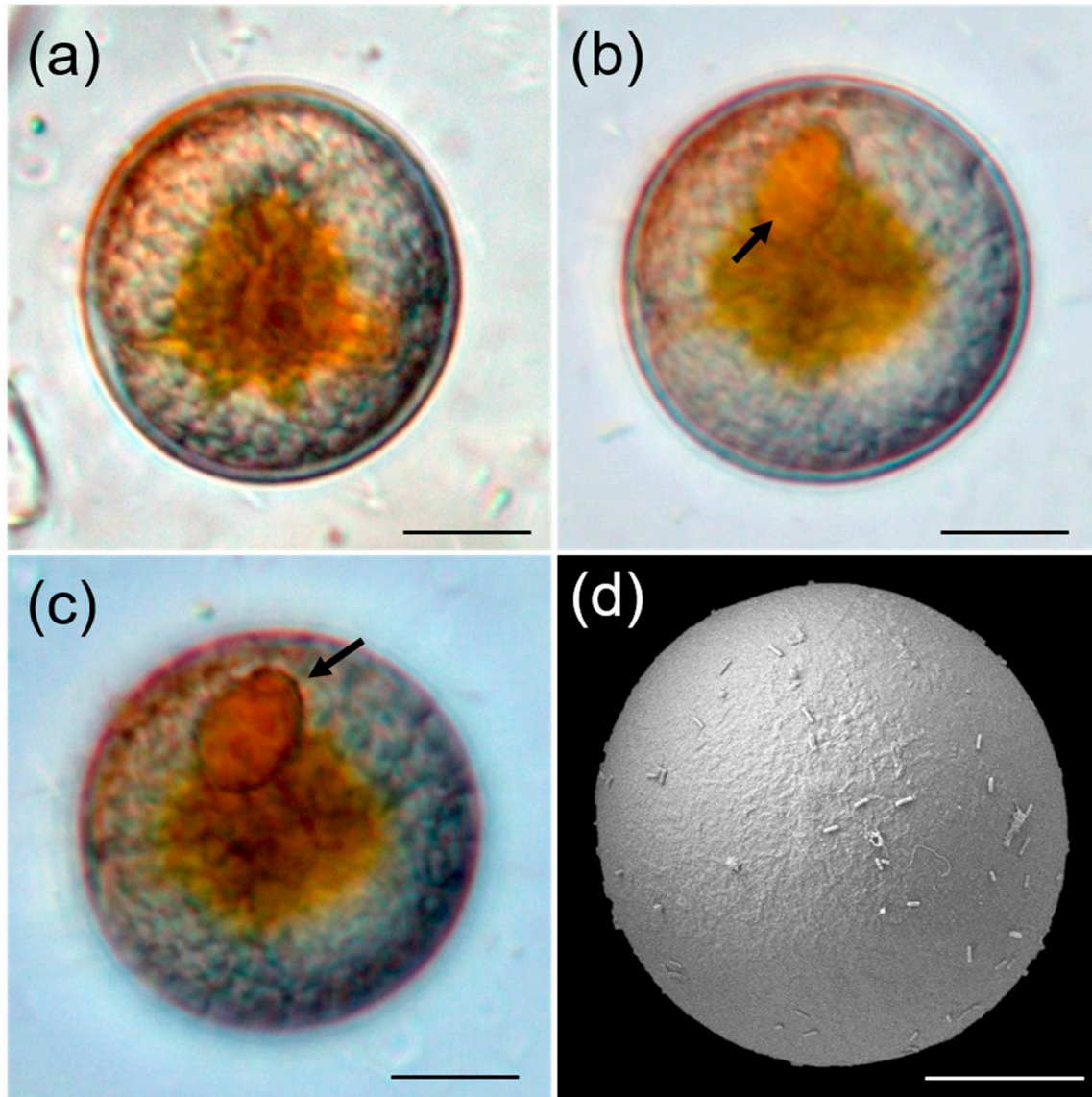


**Figure 3.** Light and scanning electron micrographs of cysts of *Bysmatrum subsalsum* strain LIMS-2685. (a) Light micrographs of spherical cyst. (b,c) Light micrographs of cysts showing large, orange, accumulation body (arrows). (d) Scanning electron micrograph showing a smooth organic wall without any ornamentation. Scale bars = 5  $\mu\text{m}$ .

### 3.2. Molecular Phylogeny

Bayesian inference (BI) and maximum likelihood (ML) based on the concatenated SSU and LSU rRNA gene sequences yielded similar phylogenetic trees. The genus *Bysmatrum* was a monophyletic group, with maximum support (Figure 4). *Bysmatrum arenicola* was the base of *Bysmatrum* species, and *B. subsalsum* was branched from *B. gregarium*, with moderate supports (BT/PP = 68/0.92). Two ribotypes (ribotype A and B) of *B. subsalsum* were identified; ribotype A was comprised only of strains from the Mediterranean Sea with maximum support (BT/PP = 100/1.00), whereas ribotype B included the strains from China, Malaysia, the French Atlantic and Korea. *Bysmatrum austrarium* (HG321) was nested between the two ribotypes. In ribotype B, the Korean strains of *B. subsalsum* were closely related to the Malaysian strain (TBBYS03) (BT/PP = 80/1.00).

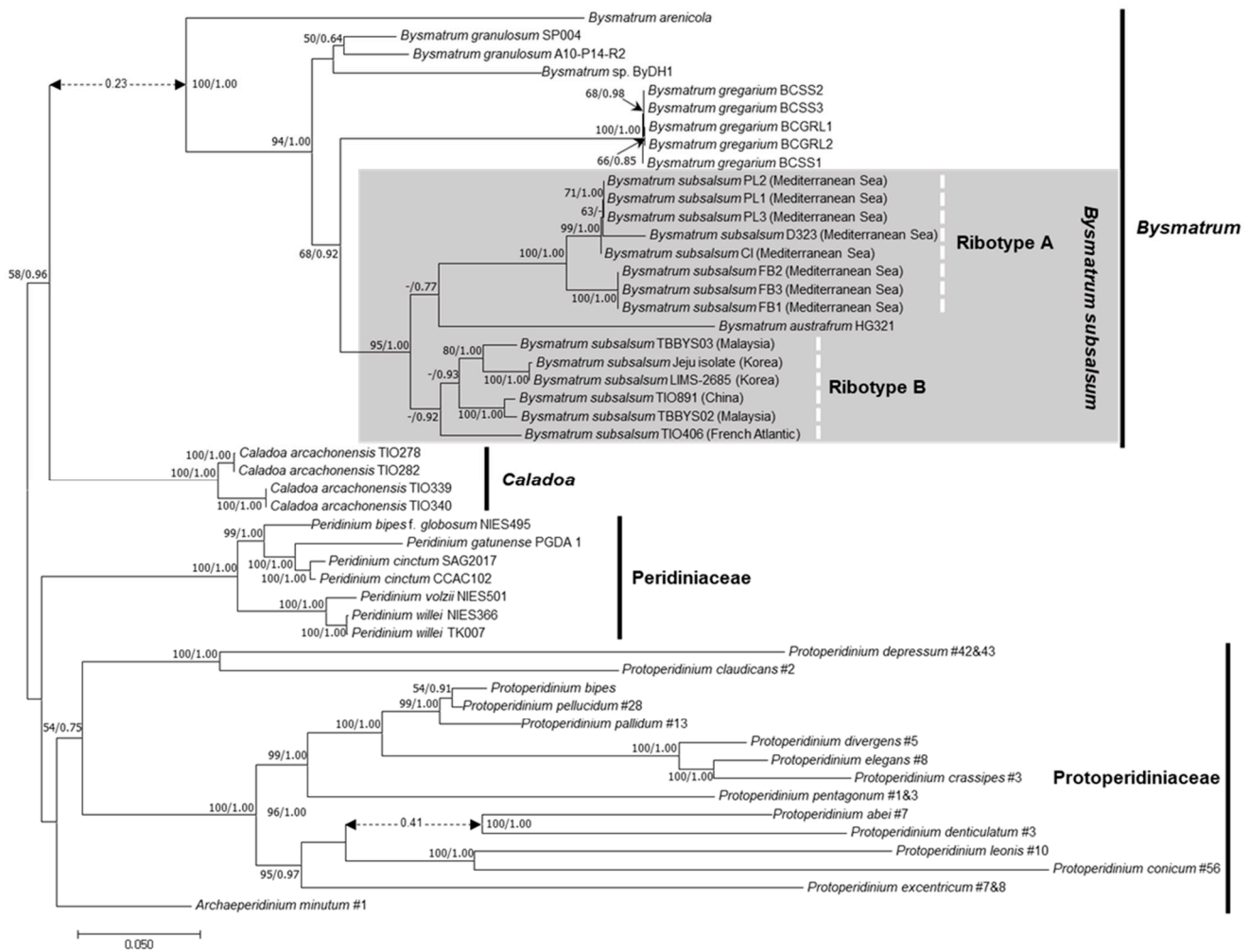


**Figure 4.** Phylogeny of *Bysmatrum subsalsum* inferred from concatenated SSU and partial LSU rRNA gene sequences using maximum-likelihood (ML). Ribotypes are labeled according to designations by Luo et al. [8]. Numbers on branches are statistical support values to clusters on the right of them (left: ML bootstrap support (BT) values; right: Bayesian posterior probabilities (PP)). Bootstrap support values > 50% and Bayesian posterior probabilities > 0.7 are shown. Branch lengths are drawn to scale, with the scale bar indicating the number of nucleotide substitutions per site.

#### 4. Discussion

##### 4.1. Morphological Comparisons of Korean Isolates of *Bysmatrum subsalsum* with Other Isolates of *B. subsalsum*, and *B. austrafurum*

According to Anglès et al. [7] and Luo et al. [8], the genetic sequences of *B. subsalsum* show large intraspecific differences, clustering two well-differentiated clades (ribotype A and B). The two clades of *B. subsalsum* based on SSU and LSU sequences were also shown in this study, and the Korean isolates of *B. subsalsum* were nested in the ribotype B and clustered with the isolates from China, Malaysia and the French Atlantic (Figure 4). The Korean isolates of *B. subsalsum* were morphologically characterized by the separation of plates 2a and 3a, the tear-shaped APC, an elongated rectangular 1a plate and the general morphology, such as cell size, plate ornamentation and nucleus position, which coincides with that of *B. subsalsum* in previous studies (Luo et al. [8] and reference therein). Luo et al. [8] reported the differences in the number of sulcal lists among strains of *B. subsalsum* in two clades; the French strain has the right sulcal list (Three sulcal lists), whereas the Malaysian strains are characterized by the absence of the right sulcal list (Two sulcal lists). In Korean strains, the right sulcal list was not present. In addition, the number of sulcal lists varied among specimens collected from other geographical regions [16–19]. Anglès et al. [7] concluded that despite a certain degree of morphological variation (such

as cell size, APC morphology and size, and cingulum displacement), cells from the two clades of *B. subsalsum* exhibit similar morphological characteristics. Luo et al. [8] also confirmed the morphological similarities in the Malaysian and French strains of *B. subsalsum*. Consequently, the prominent morphological characteristics for clarifying the two clades of *B. subsalsum* still remain unclear.

Recently, Luo et al. [20] recorded *B. australum* between two clades of *B. subsalsum*, with strong support in the phylogeny, which is in agreement with our result. *Bysmatrum australum* was first described by Dawut et al. [6]. This species has a typical plate of Po, X, 4', 3a, 7'', 6C, 4S, 5''', 2'''' for the genus *Bysmatrum* and is morphologically characterized by dimensions of 25–45 µm long and 20–42.5 µm wide, arranged reticulation in the thecal plates, the possession of an equatorially positioned cingulum and a cingulum displaced by a distance exceeding its own width. Based on these morphological features, Dawut et al. [6] reported that *B. australum* is similar to *B. subsalsum*, and concluded that *B. australum* can be distinguished from *B. subsalsum* by differences in cell size, the shape of the APC and apical plate 1'. However, cell sizes recorded in *B. australum* were recorded in the other specimens of *B. subsalsum* (see Table 2 in Luo et al. [8]), and the shapes of the APC and apical plate 1' of *B. australum* quite resembled those of Korean isolates and the specimens of *B. subsalsum* recorded by Luo et al. [8]. In addition, although Dawut et al. [6] did not consider the absence or presence of the right sulcal list, *B. australum* does not have the right sulcal list in their description. Consequently, it is quite difficult to distinguish *B. subsalsum* from *B. australum*, based on their morphological features. Nevertheless, different types of eyespots have been reported in *B. subsalsum* and *B. australum* [6,8]. Based on the types of eyespots suggested by Moestrup and Daugbjerg [21], *B. subsalsum* has the Type B eyespot, whereas *B. australum* presents the Type A eyespot. This may be a useful characteristic for distinguishing *B. subsalsum* from *B. australum*. However, as the Type A eyespot has not been reported in other *Bysmatrum* species, such as *B. granulatum* and *B. gregarium*, more isolates of *B. australum* need to be examined for clarifying the type of eyespot within *Bysmatrum* species.

#### 4.2. Morphology of *Bysmatrum subsalsum* Cyst

Cyst morphology can be helpful to understand the diversity within the genus (e.g., Li et al. [22]). In *Bysmatrum* species, a cyst–theca stage relationship has only been established through germination experiments for Mediterranean *B. subsalsum* [7]. Two types of cysts of *B. subsalsum* have been described in culture and sediments; in the culture spherical to ovoidal cysts without any ornamentations were observed [7,19], whereas cysts with the typical plate pattern, which are morphologically similar to vegetative cells of *B. subsalsum*, were identified in sediments [8,23]. In our study, the spherical cysts were also observed from the culture. *Bysmatrum subsalsum* from the Mediterranean Sea (ribotype A) could produce both cyst types in culture [7,19], and from the French strain of *B. subsalsum* (ribotype B), only cysts with the thecal plate were described [8]. In previous studies, differences in cyst types have been recorded between cultures and natural sediments. For example, unarmored dinoflagellate *Margalefidinium polykrikoides* (formerly *Cochlodinium polykrikoides*) produced two different types of cyst (a spherical cyst without ornamentation in culture and an ornamented cyst in sediments) [24,25]. Tang and Gobler [24] suggested that the ornaments and spines of *M. polykrikoides* might be caused by biotic or chemical processes in sediments. However, this does not seem to be in accordance with *B. subsalsum*, because two different types of cysts were reported in sediments.

Similar morphological features between cyst and vegetative cell of unarmored dinoflagellate *M. polykrikoides* have been reported [26,27], and the cyst was identified as a temporary cyst that can be the short-term stage. The temporary cyst of *M. polykrikoides* is surrounded by a transparent and thin hyaline membrane, indicating in sediments the unarmored temporary cysts may be destroyed because of geochemical processes related to organic matter degradation or the attack of viruses or bacteria into the cell. However, temporary cysts with thecal plates (armored cyst) (such as cyst of *B. subsalsum*) may be

protected from the environmental conditions in sediments. If so, the cyst with typical thecal plates of *B. subsalsum* from sediments or culture may be temporary, because the resting cysts of dinoflagellate usually have distinct morphological features that can be distinguished from their vegetative cell (e.g., Matsuoka and Fukuyo [28]).

#### 4.3. Phylogenetic Position of *Bysmatrum subsalsum*

In the phylogenetic tree, the Korean isolates within *B. subsalsum* were nested in the ribotype B consisting of the isolates from China, Malaysia and the French Atlantic, whereas the ribotype A includes only the isolates from the Mediterranean Sea. Iwataki et al. [29] documented that in the phylogenetic tree for *M. polykrikoides* isolates, the ribotypes can be useful for characterizing the geographical distribution pattern of *M. polykrikoides*. In our study, the ribotype A also represents the isolates of *B. subsalsum* from the Mediterranean Sea, which is in agreement with the conclusion by Iwataki et al. [29]. However, the ribotype B is a mixture of isolates originated from different geographic regions, although it mostly includes the Asian isolates. This indicates that the cells originating from France might be transferred from the Asian areas. Benthic dinoflagellates such as *Bysmatrum* species usually have a restricted distribution, possibly because of benthic, epiphytic behavior. Nevertheless, *B. subsalsum* has been reported from various samples, including plankton samples, and their resting cysts are also present in the sediments (Luo et al. [8] and reference therein). This suggests that the vegetative cells and resting cysts of *B. subsalsum* can artificially be introduced into other coastal areas, possibly caused by ballast ship waters (e.g., Hallegraeff [30]).

Since the discovery of two ribotypes of *B. subsalsum*, Luo et al. [20] identified *B. austrafurum* between two clades of *B. subsalsum* in a phylogenetic tree based on concatenated SSU and LSU rDNA sequences, which is in agreement with our result. In the phylogenetic tree, *B. subsalsum* and *B. austrafurum* were grouped, with strong support (BT/PP = 95/1.00) (Figure 4), indicating that the two species may be conspecific. This result can be supported by morphological similarity between the two species. However, as there are differences in the types of eyespots between the two species, *B. subsalsum* can also be a species that distinguished from *B. austrafurum*. If so, it is possible that *B. subsalsum* is not monophyletic. This finding supports the idea that there is cryptic diversity within *B. subsalsum* [7].

#### 4.4. Environmental Conditions in Relation to the Growth of *Bysmatrum subsalsum*

Although *Bysmatrum* species are considered benthic dinoflagellates, the occurrence of *B. subsalsum* has been reported in the plankton, with floating detritus and on sand and macroalgae [18]. Luo et al. [8] recorded *B. subsalsum* in plankton and sediment samples, and Anglès et al. [7] found *B. subsalsum* in mangrove detritus and salt marshes. In Korean isolates of *B. subsalsum*, the species is considered to inhabit tidal pools, and *B. austrafurum* was also discovered in tidal pools in South Africa [6]. In comparison with *B. subsalsum*, other *Bysmatrum* species, such as *B. teres*, *B. granulosum*, *B. arenicola* and *B. gregarium* have been reported in the restricted habitats (Luo et al. [8] and reference therein). This indicates that *B. subsalsum* in contrast to other *Bysmatrum*, may have broad environmental tolerance and a worldwide distribution.

Environmental conditions in relation to the growth of *B. subsalsum* have been rarely reported. Anglès et al. [7] documented that, based on the occurrence of *B. subsalsum* reported in previous studies, the species has a wide salinity tolerance and is able to grow under a wide range of sea water temperatures, with a preference for salinities > 30 and temperatures > 20 °C. López-Flores et al. [31] recorded that the cell abundances of *B. subsalsum* (as *Scrippsiella subsalsa*) decreased sharply in October, when salinity reached values > 30 and water temperature was low (15.6 °C). In this study, however, the dense patch of *B. subsalsum* was observed at 10.5 °C, indicating that it has a wider temperature tolerance than previously known. Further studies are also needed to clarify the morphology (vegetative cell and cyst) of the genus *Bysmatrum* and, in particular, of *B. subsalsum*.

**Author Contributions:** J.S.P. and Z.L. conceived the research; J.S.P. and K.W.L. performed field work; J.S.P., Z.L., H.J.K., K.H.K., J.Y.Y., K.Y.K., H.H.S. analyzed the data; J.S.P., Z.L., H.H.S. and K.W.L. wrote and edited the manuscript. All authors have read and agreed to the published version of the manuscript.

**Funding:** This work was supported by grants from Korea Institute of Ocean Science & Technology (PE99921), the National Marine Biodiversity Institute of Korea (2021M01100), the National Research Foundation of Korea (NRF) (No. 2018R1A6A3A01012375), and by the KRIBB Research Initiative Program (KGM5232113) and the National Research Foundation of Korea (NRF) grant funded by the Korea government (MSIT) (No. 2021R1C1C1008377).

**Institutional Review Board Statement:** Not applicable.

**Informed Consent Statement:** Not applicable.

**Data Availability Statement:** Not applicable.

**Conflicts of Interest:** The authors declare no conflict of interest.

## References

1. Faust, M.A.; Steidinger, K.A. *Bysmatrum* gen. nov. (Dinophyceae) and three new combinations for benthic scrippsielloid species. *Phycologia* **1998**, *37*, 47–52. [[CrossRef](#)]
2. Horiguchi, T.; Pienaar, R.N. Validation of *Bysmatrum arenicola* Horiguchi et Pienaar, sp. nov. (Dinophyceae). *J. Phycol.* **2000**, *36*, 237. [[CrossRef](#)]
3. Ten-Hage, L.; Quod, J.-P.; Turquet, J.; Coute, A. *Bysmatrum granulosum* sp. nov., a new benthic dinoflagellate from the southwestern Indian Ocean. *Eur. J. Phycol.* **2001**, *36*, 129–135. [[CrossRef](#)]
4. Murray, S.; Hoppenrath, M.; Larsen, J.; Patterson, D.J. *Bysmatrum teres* sp. nov., a new sand-dwelling dinoflagellate from north-western Australia. *Phycologia* **2006**, *45*, 161. [[CrossRef](#)]
5. Hoppenrath, M.; Murray, S.A.; Chomérat, N.; Horiguchi, T. *Marine Benthic Dinoflagellates-Unveiling Their Worldwide Biodiversity*; E. Schweizerbartsche Verlagsbuchhandlung: Stuttgart, Germany, 2014; 276p.
6. Dawut, M.; Sym, S.D.; Suda, S.; Horiguchi, T. *Bysmatrum austrafurum* sp. nov. (Dinophyceae), a novel tidal pool dinoflagellate from South Africa. *Phycologia* **2018**, *57*, 169–178. [[CrossRef](#)]
7. Anglès, S.; Reñé, A.; Garcés, E.; Lugliè, A.; Sechi, N.; Camp, J.; Satta, C.T. Morphological and molecular characterization of *Bysmatrum subsalsum* (Dinophyceae) from the western Mediterranean Sea reveals the existence of cryptic species. *J. Phycol.* **2017**, *53*, 833–847. [[CrossRef](#)]
8. Luo, Z.; Lim, Z.F.; Mertens, K.N.; Gurdebeke, P.; Bogus, K.; Carbonell-Moore, M.C.; Vrielinck, H.; Leaw, C.P.; Lim, P.T.; Chomérat, N.; et al. Morpho-molecular diversity and phylogeny of *Bysmatrum* (Dinophyceae) from the South China Sea and France. *Eur. J. Phycol.* **2018**, *53*, 318–335. [[CrossRef](#)]
9. Jeong, H.J.; Jang, S.H.; Kang, N.S.; Yoo, Y.D.; Kim, M.J.; Lee, K.H.; Yoon, E.Y.; Potvin, E.; Hwang, Y.J.; Kim, J.I.; et al. Molecular characterization and morphology of the photosynthetic dinoflagellate *Bysmatrum caponii* from two solar saltons in western Korea. *Ocean Sci. J.* **2012**, *47*, 1–18. [[CrossRef](#)]
10. Karen, A.S.; Tangen, K. Dinoflagellates. In *Identifying Marine Diatoms and Dinoflagellates*; Tomas, C.R., Ed.; Academic Press: San Diego, CA, USA, 1996; pp. 387–584.
11. Ki, J.-S.; Han, M.-S. Molecular analysis of complete SSU to LSU rDNA sequence in the harmful dinoflagellate *Alexandrium tamarense* (Korean isolate, HY970328M). *Ocean Sci. J.* **2005**, *40*, 43–54. [[CrossRef](#)]
12. Orsini, L.; Sarno, D.; Procaccini, G.; Poletti, R.; Dahlmann, J.; Montresor, M. Toxic *Pseudo-nitzschia multistriata* (Bacillariophyceae) from the Gulf of Naples: Morphology, toxin analysis and phylogenetic relationships with other *Pseudo-nitzschia* species. *Eur. J. Phycol.* **2002**, *37*, 247–257. [[CrossRef](#)]
13. Stamatakis, A. RAxML version 8: A tool for phylogenetic analysis and post-analysis of large phylogenies. *Bioinformatics* **2014**, *30*, 1312–1313. [[CrossRef](#)] [[PubMed](#)]
14. Ronquist, F.; Teslenko, M.; van der Mark, P.; Ayres, D.L.; Darling, A.; Höhna, S.; Larget, B.; Liu, L.; Suchard, M.A.; Huelsenbeck, J.P. MrBayes 3.2: Efficient bayesian phylogenetic inference and model choice across a large model space. *Syst. Biol.* **2012**, *61*, 539–542. [[CrossRef](#)] [[PubMed](#)]
15. Darriba, D.; Taboada, G.L.; Doallo, R.; Posada, D. jModelTest 2: More models, new heuristics and parallel computing. *Nat. Methods* **2012**, *9*, 772. [[CrossRef](#)]
16. Balech, E. Tercera contribución al conocimiento del género *Peridinium* Museo Argentino de ciencias naturales ‘Bernadino Rivadavia’ e Instituto nacional de investigacion de las ciencias naturales. *Rev. Hydrobiol.* **1964**, *4*, 179–195.
17. Steidinger, K.A.; Balech, E. *Scrippsiella subsalsa* (Ostenfeld) comb. nov. (Dinophyceae) with a discussion on *Scrippsiella*. *Phycologia* **1977**, *16*, 69–73. [[CrossRef](#)]
18. Faust, M.A. Morphology and ecology of the marine benthic dinoflagellate *Scrippsiella subsalsa* (Dinophyceae). *J. Phycol.* **1996**, *32*, 669–675. [[CrossRef](#)]

19. Gottschling, M.; Soehner, S.; Zinssmeister, C.; John, U.; Plötner, J.; Schweikert, M.; Aligizaki, K.; Elbrächter, M. Delimitation of the Thoracosphaeraceae (Dinophyceae), including the calcareous dinoflagellates, based on large amounts of ribosomal RNA sequence data. *Protist* **2012**, *163*, 15–24. [[CrossRef](#)]
20. Luo, Z.; Mertens, K.N.; Nézan, E.; Gu, L.; Pospelova, V.; Thoha, H.; Gu, H. Morphology, ultrastructure and molecular phylogeny of cyst-producing *Caladoa arcachonensis* gen. et sp. nov. (Peridinales, Dinophyceae) from France and Indonesia. *Eur. J. Phycol.* **2019**, *54*, 235–248. [[CrossRef](#)]
21. Moestrup, Ø.; Daugbjerg, N. On dinoflagellate phylogeny and classification. In *Unravelling the Algae: The past, Present, and Future of Algal Systematics*; Brodie, J., Lewis, J., Eds.; CRC press: Boca Raton, FL, USA, 2007; pp. 215–230.
22. Li, Z.; Mertens, K.N.; Gottschling, M.; Gu, H.; Söhner, S.; Price, A.M.; Marret, F.; Pospelova, V.; Smith, K.F.; Carbonell-Moore, C.; et al. Taxonomy and Molecular Phylogenetics of Ensiculiferaceae, fam. nov. (Peridinales, Dinophyceae), with Consideration of their Life-history. *Protist* **2020**, *171*, 125759. [[CrossRef](#)]
23. Limoges, A.; Mertens, K.N.; Ruiz-Fernández, A.-C.; de Vernal, A. First report of fossilized cysts produced by the benthic *Bysmatrum subsalsum* (Dinophyceae) from a shallow Mexican lagoon in the Gulf of Mexico. *J. Phycol.* **2015**, *51*, 211–215. [[CrossRef](#)]
24. Tang, Y.Z.; Gobler, C.J. The toxic dinoflagellate *Cochlodinium polykrikoides* (Dinophyceae) produces resting cysts. *Harmful Algae* **2012**, *20*, 71–80. [[CrossRef](#)]
25. Li, Z.; Han, M.-S.; Matsuoka, K.; Kim, S.-Y.; Shin, H.H. Identification of the resting cyst of *Cochlodinium polykrikoides* Margalef (Dinophyceae, Gymnodiniales) in Korean coastal sediments. *J. Phycol.* **2015**, *51*, 204–210. [[CrossRef](#)]
26. Shin, H.H.; Li, Z.; Yoon, Y.H.; Oh, S.J.; Lim, W.-A. Formation and germination of temporary cysts of *Cochlodinium polykrikoides* Margalef (Dinophyceae) and their ecological role in dense blooms. *Harmful Algae* **2017**, *66*, 57–64. [[CrossRef](#)]
27. Li, Z.; Matsuoka, K.; Shin, H.H. Revision of the life cycle of the harmful dinoflagellate *Margalefidinium polykrikoides* (Gymnodiniales, Dinophyceae) based on isolates from Korean coastal waters. *J. Appl. Phycol.* **2020**, *32*, 1863–1873. [[CrossRef](#)]
28. Matsuoka, K.; Fukuyo, Y. *Technical Guide for Modern Dinoflagellate Cyst Study*; Japan Society for the Promotion of Science: Tokyo, Japan, 2000; pp. 1–29.
29. Iwataki, M.; Kawami, H.; Mizushima, K.; Mikulski, C.M.; Doucette, G.J.; Relox, J.R.; Anton, A.; Fukuyo, Y.; Matsuoka, K. Phylogenetic relationships in the harmful dinoflagellate *Cochlodinium polykrikoides* (Gymnodiniales, Dinophyceae) inferred from LSU rDNA sequences. *Harmful Algae* **2008**, *7*, 271–277. [[CrossRef](#)]
30. Hallegraeff, G.M. Transport of toxic dinoflagellates via ships' ballast water: Bioeconomic risk assessment and efficacy of possible ballast water management strategies. *Mar. Ecol. Prog. Ser.* **1998**, *168*, 297–309. [[CrossRef](#)]
31. López-Flores, R.; Garcés, E.; Boix, D.; Badosa, A.; Brucet, S.; Masó, M.; Quintana, X.D. Comparative composition and dynamics of harmful dinoflagellates in Mediterranean salt marshes and nearby external marine waters. *Harmful Algae* **2006**, *5*, 637–648. [[CrossRef](#)]